

Department of Obstetrics and Gynecology¹, The Second Affiliated Hospital and Yuying Children's Hospital of Wenzhou Medical University; The Seventh People's Hospital of Wenzhou², Wenzhou, Zhejiang, China

DCLK1 might be a therapeutic target of osthole against cervical cancer

LIULIU PAN^{1,#}, XIAODAN ZHANG^{2,#}, DANHAN WANG¹, MIN HUANG¹, QIUSUI HUANG¹, PING DUAN¹, JIE MEI^{1,*}

Received June 4, 2021, accepted July 9, 2021

*Corresponding author: Jie Mei, The Second Affiliated Hospital and Yuying Children's Hospital of Wenzhou Medical University, Wenzhou 325027, Zhejiang, China
205162@wzhealth.com

#These authors contributed equally to this work.

Pharmazie 76: 503-506 (2021)

doi: 10.1691/ph.2021.1641

Discovering compounds with anti-cervical cancer effect and clarifying their targets will help promoting the precise treatment of cervical cancer. The present study intended to clarify the effect of osthole on cervical cancer cells, and to explore the possibility of DCLK1 as its target. Annexin V-PE staining and flow cytometry methods were used to determine cell apoptosis. Meanwhile, apoptosis related biomarkers were probed by immunoblotting. The MTT assay was employed to study the effect of osthole in combined with or without LRRK2-IN-1 (a DCLK1 inhibitor) on cell proliferation. Then, combination index was determined. To examine the interaction of osthole with DCLK1, molecular docking was carried out. Based on the biological database from cBioPortal, the association between DCLK1 and clinical manifestations of cervical cancer were evaluated. The results showed that osthole can significantly induce apoptosis of HeLa and Me-180. When combined with LRRK2-IN-1, the effect of osthole on cell proliferation was antagonized, suggesting that it might competitive binding to DCLK1. Furthermore, molecular docking showed that osthole interacts with Val468 residues of DCLK1 to form hydrogen bonds. The analysis of database showed that DCLK1 frequently mutant and deleted in cervical cancer, and is related to cell survival, tumor progression and recurrence. However, no obvious correlations were found between DCLK1 and lymphatic metastasis/differentiation. In conclusion, osthole significantly inhibits the survival of cervical cancer cells. It's probably target DCLK1 mechanistically via interacting with Val468. DCLK1 could be a potential therapeutic target for cervical cancer.

1. Introduction

Cervical carcinoma is one of the most common gynecologic tumors of the female reproductive system (Miller et al. 2020), while 80 % newly diagnosed patients come from developing countries, where the effective screening system is incomplete (Grema et al. 2019; Miller et al. 2020). Although surgery is the best strategy for treating cervical cancer, adjuvant therapies are still used to improve patients' living qualities or even to extend their life span (Cohen et al. 2019; Gadducci and Cosio 2020). Adjuvant therapy, including radiotherapy and chemotherapy, usually brings hardly tolerable toxicity and side effects. Therefore, there is an urgent need to discover and develop potent targeted drug therapy.

About two-thirds of anti-tumor medicines are derived from natural products (Mishra and Tiwari 2011). Osthole, 7-methoxy-8-(3-methyl-2-butenyl)-2H-1-benzopyran-2-one, is an extensively studied compound with diverse pharmacological effects, including antibacterial, insecticidal, anti-tumor properties (Zhang et al. 2015; Zhou et al. 2008). Osthole can potently inhibit the proliferation of many types of tumor cells, involving osteosarcoma, breast cancer, cervical cancer and non-small cell lung cancer (Che et al. 2018; Ding et al. 2014; Xu et al. 2011; Yang et al. 2010). Multi-drug resistance could also be reversed when osthole was co-administered (Wang et al. 2016). Mechanistically, osthole exerts its biological effects *via* regulating the transduction of multiple signaling pathways, including PI3K/AKT/mTOR, NF- κ B (Ding et al. 2013; Kao et al. 2012).

Although the effect of osthole on cervical cancer has previously been determined, the direct pharmacological target has not been unveiled yet. Given the data from the literature which had demonstrated that doublecortin-like kinase 1 (DCLK1) is associated with the development of cervical cancer (Qu et al. 2019; Wang et al.

2018). Herein, we intended to explore the possibility of DCLK1 as a target of osthole, and to develop the relationship between DCLK1 expression level and progression of cervical cancer. It would provide preliminary data for target validation, and provide an effective chemical structure core for drug designing.

2. Investigations and results

2.1. Osthole and LRRK2-IN-1 remarkably induce the apoptotic death of cervical cancer cells

We applied annexin V/PE staining to determine the effects of osthole and LRRK2-IN-1 (LRRK, a DCLK1 inhibitor) on survival of cervical cancer cell lines, including HeLa and Me-180. As Figs. 1A-C show, osthole significantly induced HeLa and Me-180 cells apoptotic death dose-dependently. But it has a higher potency in HeLa than in Me-180 cells. Besides, LRRK induced 25.09 % cell death in HeLa, while no significant difference was observed in Me-180. What's more, approaching 90 % cells of HeLa was made apoptotic by osthole at 160 μ M. In consistence, cleaved PARP, an apoptosis biomarker, was significantly upregulated by osthole at 180 mM both in HeLa and Me-180 (Fig. 1D). Meanwhile, LRRK remarkably upregulated the level of cleaved-PARP in HeLa, which is distinguished from that in Me-180.

2.2. Osthole antagonizes with LRRK in suppressing the proliferation of cervical cancer cell lines

As shown in Figs. 2A and B, the half inhibitory concentrations (IC_{50}) of osthole on HeLa and Me-180 were $45.01 \pm 3.91 \mu$ M, $88.95 \pm 0.13 \mu$ M, respectively, while it was $8.35 \pm 1.62 \mu$ M and $10.29 \pm 0.18 \mu$ M for LRRK accordingly. Next, we combined these

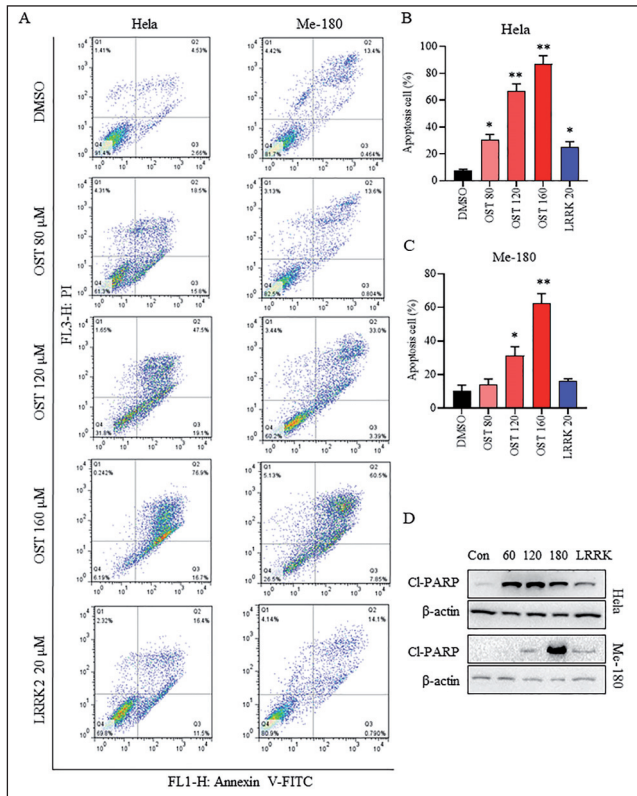


Fig. 1: Osthole induces apoptotic death of HeLa and Me-180. (A) HeLa and Me-180 were treated with osthole and LRRK for 48 h, then the cells were subjected to flow cytometry using Annexin V-PE staining assay. (B-C) The percentages of apoptotic cells were determined using flowjo software and plotted. (D) The lysates were prepared and subjected to immunoblotting assay for cleaved PARP. β-actin was considered as loading control. Osthole or LRRK vs DMSO, * $P < 0.05$, ** $P < 0.01$.

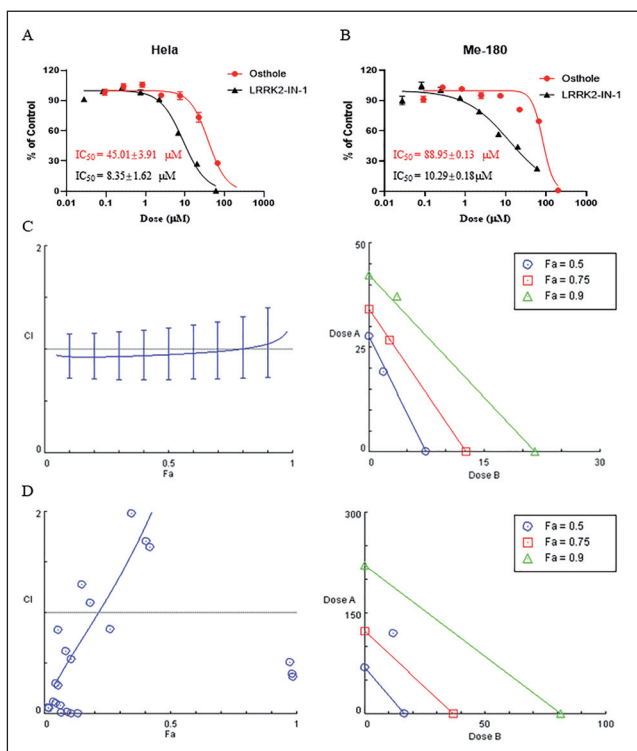


Fig. 2: The effects of osthole combined with or without LRRK on cell proliferations of HeLa and Me-180. (A-B) HeLa and Me-180 were seeded into 96-well plate, and treated with osthole or LRRK2-IN-1 for 72 h. Then, the plates were subjected to MTT assay. Finally, the inhibitory curves were plotted accordingly, and IC_{50} values were figured out. (C-D) Osthole and LRRK was combined at the constant ration of 10:1. After 72 h treatment, the cells were subjected to MTT method. The CI was obtained by using Compusyn software.

two compounds to examine their effects on cell proliferation. The results demonstrated that when the inhibition rate (Fa, fraction of system affected) was greater than 80%, the combination index is greater than 1, indicating these two compounds have an antagonistic effect (Figs. 2C and D). From the isobolograms curve, the same conclusion can be drawn. The collective data suggested that osthole and LRRK may have the same target.

2.3. Osthole forms a stable hydrogen bond with Val468 in the active pocket of DCLK1

Next, molecular docking assay was applied to investigate the direct interaction between osthole and DCLK1. A hydrogen bond was formed between osthole and Val468 residue of DCLK1 with docking energy of 6.234 kcal/mol (Figs. 3A and B). Interestingly, the crystal structure analysis showed that Val468 and NVP-TAE684 (a DCLK1 inhibitor) also form hydrogen bonds (Fig. 3C). The interaction between Val468 and the amino nitrogen of pyrimidine is an important structure for inhibitor binding, and is highly conservative. Therefore, the collective data indicated that osthole can inhibit DCLK1 via binding with Val468.

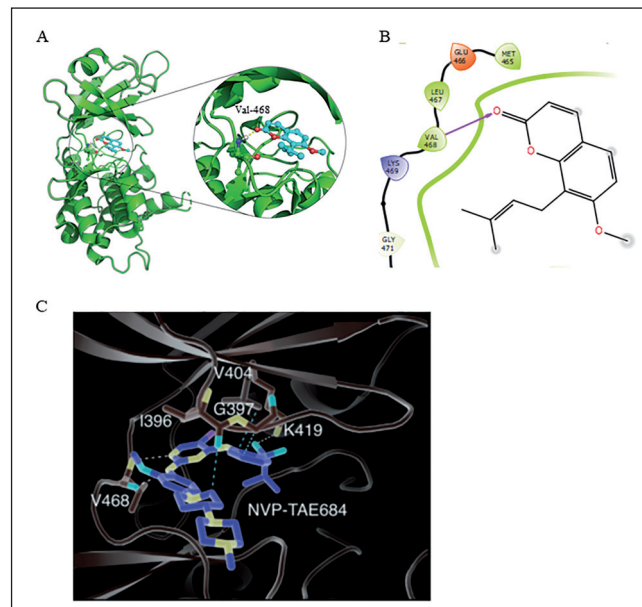


Fig. 3: Molecular docking of osthole with DCLK1. (A-B) AutoDock 4.2 was applied to set up assay as detailed indicated in the method. DCLK1 is shown in green; Osthole is shown in light blue. (C) Close up of the interaction of NVP-TAE684 with DCLK1 kinase domain (Patel et al. 2016). NVP-TAE684 is shown in blue; DCLK1 kinase domain is shown in black.

2.4. The variation of DCLK1 in cervical cancer and its correlation with clinical phenotype

In order to study the variation characteristics of DCLK1 in tumors, we used the cBioPortal for cancer genomics platform (<http://www.cbioportal.org/>) to analyze the mutant profile of DCLK1 and according frequency in various types of cancer (Cerami et al. 2012; Gao et al. 2013). As shown in Fig. 4A, nucleic acid mutation was the most frequently occurring type. In cervical cancer, mutations and deletions were the main features. Subsequently, we further used the transcriptome sequencing data from the platform to analyze the expression differences of DCLK1 between cervical adenocarcinoma and cervical squamous cell carcinoma. The results showed that although the expression level of DCLK1 in cervical squamous cell carcinoma was higher than that in adenocarcinoma, there was no statistical difference between them (Fig. 4B). To further explore the relationships between DCLK1 and clinical manifestations, we separately analyzed the recurrence rate, lymphatic metastasis, and degree of differentiation. As shown in Figs. 4C-E, the expression of DCLK1 showed an upward trend in the recurrence and progres-

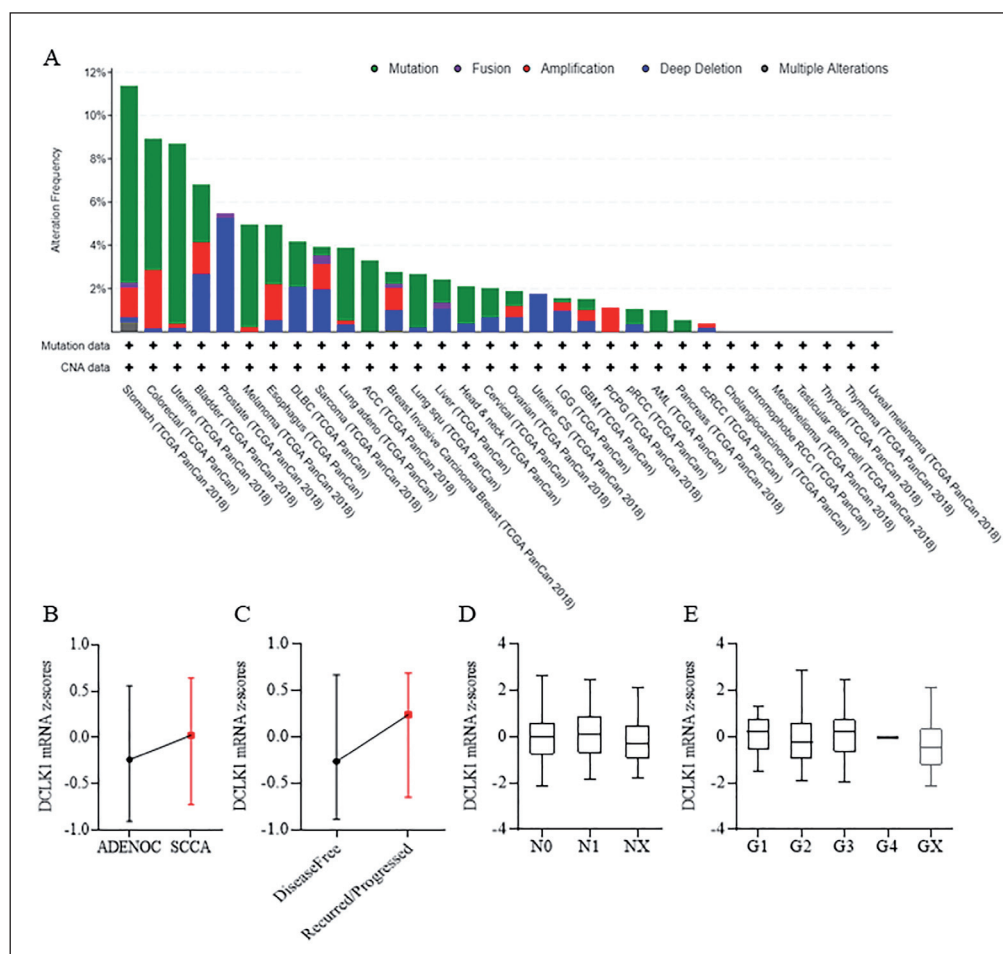


Fig. 4: The characteristic profile of DCLK1 in cervical cancer. (A) Variation characteristics of DCLK1 was analyzed based on data from cBioPortal for cancer genomics. (B-E) The correlation of DCLK1 with clinical manifestations of cervical cancer was analyzed and plotted.

sion of cervical cancer ($P>0.05$). But there were no significant differences observed among groups in the lymph node metastasis and differentiation.

3. Discussion

Cervical cancer is the gynecologic malignancy of female reproductive system with the highest lethality and incidence. Etiological studies had shown that nearly 95% of the morbidity is related to the chronic inflammation caused by HPV infection (Schiffman et al. 2011; Uyar and Rader 2014). Although it is possible to prevent cervical cancer through vaccination, the number of people vaccinated is still small. After being diagnosed, surgery and adjuvant therapy can improve the patient's quality of life and prolong their life span. With the development of precision medicine, the genomic and proteomic characteristics of cervical cancer have been revealed. The characteristic mutations of *SHKBP1*, *ERBB3*, *CASP8*, *HLA-A* and *TGFBR2* in cervical cancer have also been identified (Uyar and Rader 2014). These achievements undoubtedly provide a basis for promoting the precise treatment of cervical cancer and targeted drug design.

Natural compounds are an important resource of chemotherapeutic drugs. Due to their low toxicity, they have been a research hotspot for a long period. Osthole has widely been investigated. Although some studies have reported the effect of osthole on cervical cancer cells mechanistically through blocking ATM/NF- κ B, its specific target is still undetermined (Che et al. 2018). In terms of efficacy on inhibiting proliferation and inducing apoptosis, the results of this study are consistent with the data published previously. In addition, we found that osthole had an antagonistic effect on LRRK2-IN-1 and this implies that osthole has the same target as LRRK2-IN-1. Moreover, LRRK2-IN-1 is a DCLK1 inhibitor. Therefore, we hypothesize that DCLK1 is the direct target of osthole. Subsequently, molecular docking provided us with more

evidence, and the results showed that osthole and Val468 residues of DCLK1 can form a hydrogen bond. This structure is necessary for the binding of DCLK1 to the substrate molecule, indicating that osthole and DCLK1 have a structural basis for mutual binding. The above results indicate that DCLK1 may be the direct target of osthole to exert its anti-cervical cancer effect. However, it still needs further study to validate the present preliminary data.

HeLa cells are adenocarcinoma, and Me180 cells are squamous carcinoma cells. Based on our data, HeLa cells are much more sensitive to osthole than Me180. But this effect is not proportional to the abundance of DCLK1. Using biological database analysis, we found that there is no statistical difference in the transcription level of DCLK1 between cervical adenocarcinoma and squamous cell carcinoma. Interestingly, HeLa cells are HPV18-positive cells, while Me180 cells contain HPV33. Whether the type of HPV determines the sensitivity to DCLK1 inhibitors still needs further research.

DCLK1 has high homology with doublecortin (DCX) gene sequence, and is highly expressed together with DCX during the development and migration of cerebral cortical neurons (Lin et al. 2000). Studies have shown upregulated expression of DCLK1 in cervical cancer, gastric cancer, colon cancer, pancreatic cancer, etc (Qu et al. 2019). However, the specific role and regulatory mechanism of DCLK1 in cervical cancer still needs to be determined.

4. Experimental

4.1. Reagents

Osthole was obtained from Aladdin (purity $\geq 99\%$, Shanghai, China), and LRRK2-IN-1 was purchased from Selleckchem (Houston, Texas, USA). The compounds were dissolved in diethyl sulfoxide (DMSO, Sigma, CA, USA) to make a 20 mM stock solution. 1-(4,5-Dimethylthiazol-2-yl)-3,5-diphenylformazan (MTT) powder was purchased from Sigma (CA, USA).

4.2. Cell culture

HeLa, and Me-180 cell lines were provided by the Shanghai Institute of Biochemistry and Cell Biology (Shanghai, China). HeLa cells were cultured in Eagle's minimal essential medium (EMEM). McCoy's 5A medium was used to culture Me-180 cells. Cultural medium was supplemented with 10 % fetal bovine serum (FBS) and penicillin-streptomycin (Gibco, MA, USA). The cells were maintained in 37 °C incubator with 5 % CO₂.

4.3. Flow cytometry assay

After incubating with osthole or LRRK for 48 h, Annexin V-PE apoptosis detection kit (Beyotime, Beijing, China) was used to determine the apoptosis according to the manufacturer's instruction. Finally, flow cytometry was performed on BD FACScalibur. Data was assessed using FlowJo software.

4.4. Immunoblotting assay

The total protein was extract from the cells by using NuPAGE LDS sample buffer (ThermoFisher, MA, USA). Then, the samples were subject to electrophoresed and transferred to PVDF membrane. Thereafter, the membrane was blocked using 5% non-fat milk for 2 h. The blot was incubated with the primary antibody at 4 °C overnight. As following, HRP-conjugated secondary antibody was incubated with the membrane for another 2 hours. Subsequently, the blot was visualized using ImmuneStar HRP ECL kit (Biorad, CA, USA) on imager. Primary antibody, Cleaved PARP, was obtained from cell signaling technology (MA, USA). The secondary antibody was obtained from Shanghai Yeasen Biotechnology Company (Shanghai, China).

4.5. Determination of cell viability

MTT assay was applied to evaluate the viability of cells. The cells were seeded into 96-well plates as 1000 cells/well at the total volume of 150 µL. After culturing for overnight, 50 µL osthole or DMSO was added into the well to the final concentration of 6.26, 12.5, 25, 50, 100, 200, 400 and 800 µM. While LRRK2-IN-1 was added into the wells to the final concentration of 60, 20, 6.67, 2.22, 0.74, 0.25, 0.082 and 0.027 µM. After incubation for another 72 h, MTT was added in the medium to the final concentration of 1 mg/mL and incubated for extra 4 h. The formed formazan was dissolved using DMSO (150 µL/well), then the solution was subjected to absorbance measure using a microplate reader at 570 nm.

4.6. Combination index (CI) determination

Osthole and LRRK were mixed at the constant ratio of 10:1. The cells were treated for 72 h, then subjected to MTT assay as being indicated above. Compusyn software was used to determine the CI according to the instruction from the manufactory (Chou, 2006, 2010).

4.7. Molecular docking

The crystal structure of DCLK1 (5JZJ) was obtained from Protein Data Base. Pre-processing was performed on PyMol by removing water molecule, ligands and addition of hydrogen atoms. The docking of DCLK1 and osthole were set up on AutoDock 4.2, with default parameters. The complex with lowest docking energy was extracted.

4.8. Statistical analysis

The results were shown as means±SD. GraphPad Prism 5.0 (San Diego, CA, USA) was used to draw figure and statistical analysis. Comparison among groups were assess of statistical significance by non-parametric Kruskal-Wallis test followed by Dunn's post hoc test. $P < 0.05$ was considered statistically significant.

Acknowledgement: Financial support was provided by Wenzhou science and Technology Bureau project (Y20180267).

Conflicts of interest: All the authors declare no competing financial interest.

References

Cerami E, Gao J, Dogrusoz U, Gross BE, Sumer SO, Aksoy BA, Jacobsen A, Byrne CJ, Heuer ML, Larsson E, Antipin Y, Reva B, Goldberg AP, Sander C, Schultz N (2012) The cBio cancer genomics portal: an open platform for exploring multidimensional cancer genomics data. *Cancer Discov* 2: 401–404.
 Che Y, Li J, Li Z, Li J, Wang S, Yan Y, Zou K, Zou L (2018) Osthole enhances anti-tumor activity and irradiation sensitivity of cervical cancer cells by suppressing ATM/NF-kappa B signaling. *Oncol Rep* 40: 737–747.

Chou TC (2006) Theoretical basis, experimental design, and computerized simulation of synergism and antagonism in drug combination studies. *Pharmacol Rev* 58: 621–681.
 Chou TC (2010) Drug combination studies and their synergy quantification using the Chou-Talalay method. *Cancer Res* 70: 440–446.
 Cohen PA, Jhingran A, Oaknin A, Denny L (2019) Cervical cancer. *Lancet* 393: 169–182.
 Ding D, Wei S, Song Y, Li L, Du G, Zhan H, Cao Y. Osthole exhibits anti-cancer property in rat glioma cells through inhibiting PI3K/Akt and MAPK signaling pathways *Cell Physiol Biochem* 32: 1751–1760.
 Ding Y, Lu XW, Hu XP, Ma J, Ding H (2014) Osthole inhibits proliferation and induces apoptosis in human osteosarcoma cells. *Int J Clin Pharmacol Ther* 52: 112–117.
 Gadducci A, Cosio S (2020) Neoadjuvant chemotherapy in locally advanced cervical cancer: Review of the literature and perspectives of clinical research. *Anticancer Res* 40: 4819–4828.
 Gao J, Aksoy BA, Dogrusoz U, Dresdner G, Gross B, Sumer SO, Sun Y, Jacobsen A, Sinha R, Larsson E, Cerami E, Sander C, Schultz N (2013) Integrative analysis of complex cancer genomics and clinical profiles using the cBioPortal. *Sci Signal* 6(269), p11.
 Grema BA, Aliyu I, Michael GC, Mafala MB (2019) Diagnosing premalignant lesions of uterine cervix in a resource constraint setting: a narrative review. *West Afr J Med* 36: 48–53.
 Kao SJ, Su JL, Chen CK, Yu MC, Bai KJ, Chang JH, Bien MY, Yang SF, Chien MH (2012) Osthole inhibits the invasive ability of human lung adenocarcinoma cells via suppression of NF-kappa B-mediated matrix metalloproteinase-9 expression. *Toxicol Applied Pharmacol* 261: 105–115.
 Lin PT, Gleeson JG, Corbo JC, Flanagan L, Walsh CA (2000) DCAMK1 encodes a protein kinase with homology to doublecortin that regulates microtubule polymerization. *J Neurosci* 20: 9152–9161.
 Miller D, Morris CP, Maleki Z, White M, Rodriguez EF (2020) Health disparities in cervical cancer: Prevalence of high-risk HPV and cytologic diagnoses according to race. *Cancer Cytopathol* 128: 860–869.
 Mishra BB, Tiwari VK (2011) Natural products: An evolving role in future drug discovery. *Eur J Med Chem* 46: 4769–4807.
 Patel O, Dai W, Mentzel M, Griffin MD, Serindoux J, Gay Y, Fischer S, Sterle S, Kropp A, Burns CJ, Ernst M, Buchert M, Lucet IS (2016) Biochemical and structural insights into doublecortin-like kinase domain 1. *Structure*, 24, 1550–1561.
 Qu D, Weygant N, Yao J, Chandrakesan P, Berry WL, May R, Pitts K, Husain S, Lightfoot S, Li M, Wang TC, An G, Clendenin C, Stanger BZ, Houchen CW (2019) Overexpression of DCLK1-AL increases tumor cell invasion, drug resistance, and KRAS activation and can be targeted to inhibit tumorigenesis in pancreatic cancer. *J Oncol* 2019: 6402925.
 Schiffman M, Wentzensen N, Wacholder S, Kinney W, Gage JC, Castle PE (2011) Human papillomavirus testing in the prevention of cervical cancer. *J Natl Cancer Inst* 103: 368–383.
 Uyar D, Rader J (2014). Genomics of cervical cancer and the role of human papillomavirus pathobiology. *Clin Chem* 60: 144–146.
 Wang D, Wang H, Li Y, Li Q (2018) MiR-362-3p functions as a tumor suppressor through targeting MCM5 in cervical adenocarcinoma. *Biosci Rep* 38: 38(3):BSR20180668.
 Wang H, Jia XH, Chen JR, Wang JY, Li YJ (2016) Osthole shows the potential to overcome P-glycoprotein-mediated multidrug resistance in human myelogenous leukemia K562/ADM cells by inhibiting the PI3K/Akt signaling pathway. *Oncol Rep* 35: 3659–3668.
 Xu XM, Zhang Y, Qu D, Jiang TS, Li SQ (2011) Osthole induces G2/M arrest and apoptosis in lung cancer A549 cells by modulating PI3K/Akt pathway. *J Exper Clin Cancer Res* 30: 33.
 Yang DP, Gu TW, Wang T, Tang QJ, Ma CY (2010) Effects of osthole on migration and invasion in breast cancer cells. *Biosci Biotechnol Biochem* 74: 1430–1434.
 Zhang ZR, Leung WN, Cheung HY, Chan CW (2015) Osthole: a review on its bioactivities, pharmacological properties, and potential as alternative medicine. *Evid Based Complem Altern Med* 2015: 919616.
 Zhou J, Sun XL, Wang SW (2008) Micelle-mediated extraction and cloud-point preconcentration of osthole and imperatorin from *Cnidium monnieri* with analysis by high performance liquid chromatography. *J Chromatogr* 1200: 93–99.